Mechanical Flocculation in Flowing Fiber Suspensions

C. F. Schmid and D. J. Klingenberg

Department of Chemical Engineering and Rheology Research Center, University of Wisconsin, Madison, Wisconsin 53706

(Received 17 August 1999)

Non-Brownian fibers commonly flocculate in flowing suspensions. A particle level simulation technique modeling fibers as chains of rods connected by hinges is developed to probe flocculation. Simulations show that flocculation can be induced solely by interfiber friction—attractive forces between fibers are not necessary. Simulated mechanical floc characteristics are consistent with experimental observations. In contrast, simulations of flocs formed by attractive forces behave qualitatively differently.

PACS numbers: 61.20.Ja, 47.55.Kf, 82.70.Dd

The flocculation of particles in viscous media is a widely encountered phenomenon. Flocculation typically results from attractive forces between particles, arising from electromagnetic (van der Waals forces), or chemical (nonadsorbed polymer depletion [1], adsorbed polymer bridging [2]) mechanisms. Here, we describe a distinct type of flocculation that occurs *without* attractive forces between particles.

Suspensions of non-Brownian fibers often become heterogeneously dispersed when sheared (Fig. 1). Understanding this flocculation is important in processing fiber-filled fluids, and may also have implications for flowing solutions of semiflexible macromolecules [3].

Mason was the first to recognize that fiber flocculation occurs under conditions where electromagnetic and chemical forces are negligible compared to hydrodynamic forces [4,5]. Others have suggested the importance of mechanical fiber features such as flexibility, irregular equilibrium shapes, and frictional contact forces [6–8], although the exact role of each is not completely understood. The process by which fibers flocculate has also not been fully elucidated. Mason [4] postulated that flocculation is a dynamic equilibrium process, with fibers continuously entering and leaving flocs, both rates being equal at steady state. Meyer and Wahren [9] proposed a physical mechanism, wherein fibers elastically deformed by the flow crowd together and interlock. Experiments support this mechanism, showing the shear modulus of fiber networks to be proportional to the bending stiffness of constituent fibers [10], and floc cohesiveness to be linked to the storage of elastic energy in fibers [11]. However, the flocculation process is difficult to observe experimentally, as fibers are small, opaque, and moving rapidly in most applications.

To systematically investigate fiber flocculation, we have developed a particle level simulation technique. Fibers are modeled as chains of rigid rods connected by hinges (Fig. 2). Equations governing the motion of a model fiber are derived from force and torque balances on each rod in a chain, with the constraint that the chain contour length is constant. Particles of interest typically have diameters D of several microns, and lengths L of a few millimeters, thus particle and fluid inertia are neglected. A brief description of the model is presented here; more details are available elsewhere [12,13].

The force and torque balances on each rod in a chain contain contributions from four sources: hydrodynamic forces and torques, elastic bending and twisting torques, interparticle forces and their moments (including friction), and constraint forces and their moments (to hold rods together in a chain). The fluid is assumed to be Newtonian, and hydrodynamic interactions between particles are neglected. Here we consider simple shear flow, $u_x = \dot{\gamma} z$. Bending and twisting torques are given by $|\boldsymbol{Y}_x| = \kappa_x(\theta_x - \theta_x^{\mathrm{eq}})$, where $x = b$ (bend), t (twist). The parameters κ_b and κ_t are related to the bending and twisting stiffness of a real fiber, respectively, by $\kappa_b l = E_Y I$ and $\kappa_t l = GJ$. Here l is the rod length used in the model fiber, E_Y and G are the Young's modulus and shear modulus of the fiber material, and I and J are the appropriate area moments of inertia. Equilibrium angles $\theta_{b,t}^{\mathrm{eq}}$ allow arbitrary equilibrium model fiber shapes to be specified. Fibers contact when the distance between surfaces s falls below a cutoff value ($s \leq R/3$), where R is the fiber radius. Short range repulsive forces $|\boldsymbol{f}^{\mathrm{rep}}| = F \exp(-20s/R)$ are applied between contacting fibers, where $F = 120\pi\mu LR\dot{\gamma}$ is chosen to prevent particles from overlapping. Contacting fibers also interact through static friction forces $|\boldsymbol{f}^{\mathrm{fric}}|$, which constrain particles to roll over one another without slipping. Static friction forces are applied at contacts

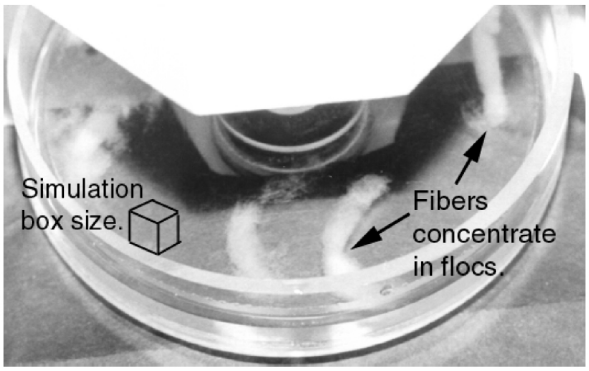

FIG. 1. Top view of fiber suspension flow between plexiglass parallel plates—highly flocculated 0.125 wt% Kraft pulp in 87% volume aqueous glycerol solution.

 0031-9007/00/84(2)/290(4)$15.00

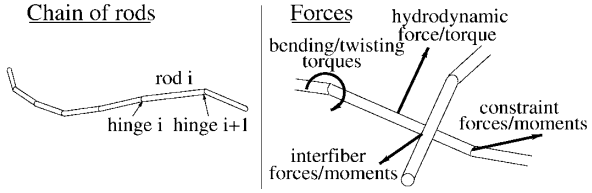

FIG. 2. Schematic of a model fiber, and the forces and torques that act on each rod.

if $|\boldsymbol{f}^{\mathrm{fric}}| \leq \mu_f^{\mathrm{stat}} |\boldsymbol{f}^{\mathrm{rep}}|$, where μ_f^{stat} is the static friction coefficient. If $|\boldsymbol{f}^{\mathrm{fric}}| > \mu_f^{\mathrm{stat}} |\boldsymbol{f}^{\mathrm{rep}}|$, contacting fibers are allowed to slide freely, mimicking a sliding friction coefficient of zero. Constraint forces holding the chain together satisfy the chain inextensibility constraint.

A simple experiment motivates the simulations. An initially homogeneous 0.125 wt. % suspension of bleached, softwood pulp fibers in 87% volume aqueous glycerol solution (viscosity $\mu = 0.1$ Pa $\cdot$ sec at 20 °C) is sheared in a 2.5 mm gap between parallel plates with the shear rate at the outer edge of the plates $\frac{\partial v_\theta}{\partial z} \equiv \dot{\gamma} = 40/\mathrm{sec}$. Fibers rapidly aggregate. After 10 sec (edge strain of 400), fibers begin to concentrate in strands oriented in the flow (θ) direction. After 30 sec, these fiber flocs densify and roll into tubes that tend to align in the vorticity (radial) direction, as shown in Fig. 1. Fibers used in this experiment have an average length of $\approx$2.5 mm and average diameter of $\approx$35 μm. Equilibrium fiber shapes are shown in Fig. 3a. A typical bending stiffness of softwood pulp fibers is $E_Y I = 8 \times 10^{-12}$ N m^2 [14].

Simulations under similar conditions show the importance of mechanical features on flocculation. The model fiber aspect ratio $r_p \equiv L/D = 70$ and dimensionless bending stiffness $\mathrm{DS} \equiv \frac{E_Y I}{\mu \dot{\gamma} L^4} = 0.050$ are specified to match experimental conditions, and the model fiber equilibrium shape (shape in the absence of flow) is helical to mimic real particles (Fig. 3b). Simulations of 0.125 vol % suspensions of 121 neutrally buoyant fibers undergoing simple shear flow are performed. An initially homogeneous suspension is sheared for a strain of 5000 in a cubic simulation box (side length = 2.5 fiber lengths). Periodic boundary conditions are applied. When particles interact through repulsive normal forces only, the suspension remains homogeneously dispersed (Fig. 4a). When the coefficient of static friction is increased to about 20, flocs form within strains of $\gamma = 500$–1000 (Fig. 4b).

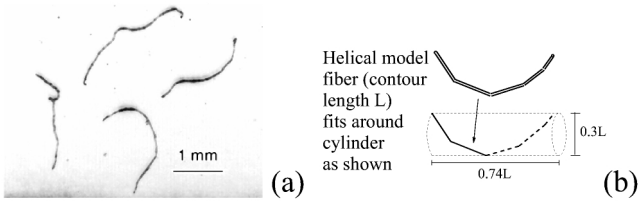

FIG. 3. (a) Equilibrium shapes of Kraft pulp fibers used in experiments, (b) model fiber equilibrium shape used in simulations.

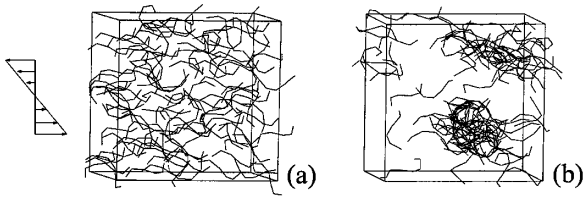

FIG. 4. Simulations of 0.125 vol % suspensions of helical fibers, $r_p = 70$, DS = 0.050: (a) static friction coefficient $\mu_f^{\mathrm{stat}} = 0$, (b) $\mu_f^{\mathrm{stat}} = 20$.

Simulations exhibit floc formation in the *absence* of attractive forces between fibers. Here, frictional interactions lead to flocculation. However, other features such as fiber equilibrium shape and fiber stiffness play roles. For example, suspensions of intrinsically straight fibers at the same concentration, aspect ratio, and stiffness as in Fig. 4 remain homogeneously dispersed, even for $\mu_f^{\mathrm{stat}} = \infty$. Suspensions of helical fibers at the same conditions as in Fig. 4b remain dispersed if the stiffness is dropped to DS = 0.0050.

To quantify fiber mass distribution, the pair distribution function $g(r)$ for fiber centers of mass (CM) is employed, where r is the distance between fiber CM. Figure 5 compares pair distribution functions for the two suspensions considered in Fig. 4. Here, $g(r)$ are time averaged after the suspension has equilibrated for a strain of 1000, and averaged over five runs with different initial configurations. Curve (b) in Fig. 5 shows that static friction forces and helical fiber equilibrium shapes lead to an increased probability of two fibers being close to one another. In contrast, without interfiber friction, $g(r) \leq 1$ [curve (a)].

The coherency of fiber flocs is thought to derive from the storage of elastic energy in the fibers. Evidence connecting floc strength and elastic energy storage is provided by experiments—for example, nylon fiber flocs disperse readily when bending stresses are diminished by heating the flocs above the nylon glass transition temperature [11]. Our simulations capture this elastic energy storage phenomenon. Model suspensions are first sheared, and

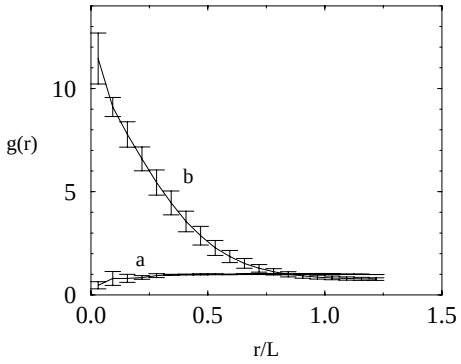

FIG. 5. Steady state fiber CM pair distribution function for 0.125 vol % suspensions of helical fibers, $r_p = 70$, DS = 0.050: (a) $\mu_f^{\mathrm{stat}} = 0$, (b) $\mu_f^{\mathrm{stat}} = 20$. [Flexible fiber CM's may coincide, so $g(0)$ isn't necessarily zero.]

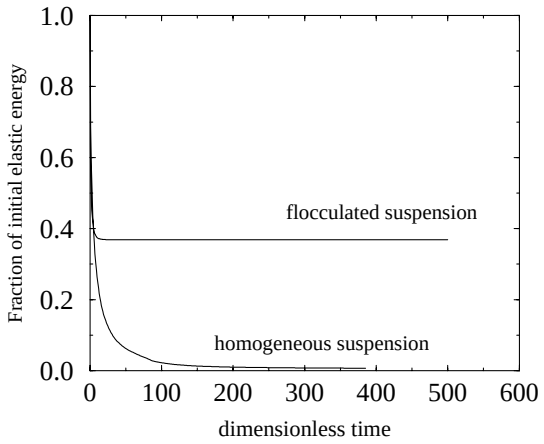

FIG. 6. Fraction of initial elastic energy stored in fibers versus dimensionless time (t/t_{scale}) after cessation of shear flow: 0.125 vol% helical fibers, $r_p = 70$, DS2 = 3.73, $\mu_f^{\text{stat}} = 20$.

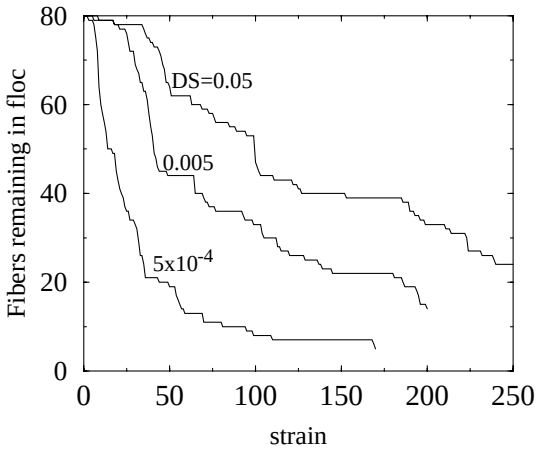

FIG. 7. Fibers remaining in a floc in unbounded shear flow as a function of strain for various fiber stiffnesses, $r_p = 70$, helical fibers, $\mu_f^{\text{stat}} = 20$.

subsequently the flow is turned off, allowing fibers to relax. Figure 6 tracks the fraction of initial elastic energy stored in the fibers as a function of dimensionless time after cessation of shear flow, where time is arbitrarily scaled by the quantity $t_{\text{scale}} = \frac{\pi\mu L^3 R}{0.45 E_Y I}$. Dimensionless bending stiffness is now defined as DS2 $\equiv \frac{E_Y I t_{\text{scale}}}{\mu L^4}$. In homogeneous suspensions, the elastic energy quickly decays to zero and fibers assume their equilibrium shapes. In flocculated suspensions, the elastic energy relaxes to a finite value, as fibers cannot revert completely to their equilibrium shapes because of contacts with other fibers.

To illustrate the importance of elastic energy in holding flocs together, we simulate the breakup of individual flocs in an infinite shear flow. Here, flocs are first formed in a simple shear flow with periodic boundaries as discussed above. Individual flocs are then removed from the suspension and placed alone in an unbounded shear flow. As fibers break from the floc, they are carried away by the flow—the diminishing population of fibers in a floc is tracked as a function of time. Figure 7 follows the breakup of a floc that originally contains 80 fibers of aspect ratio 70 for various dimensionless fiber stiffnesses. As the stiffness DS $= \frac{E_Y I}{\mu\dot{\gamma} L^4}$ decreases, flocs disperse faster. Simulations are consistent with the experimental observation that flocs are more prevalent at low shear rates and low suspending fluid viscosities (high stiffnesses) [15,16]. However, even flocs made of stiff fibers eventually break up. This supports the dynamic equilibrium hypothesis of Mason and co-workers—fibers constantly enter and leave flocs, and do not irreversibly bind to them [4].

Now we compare simulations of suspensions with attractive interfiber forces to those with frictional forces. Here, a short range attractive force $|\boldsymbol{f}^{\text{att}}| = A\exp(-10s/R)$ is applied between fibers, where $A = 120\pi\mu L R\dot{\gamma}$, along with the repulsive force $|\boldsymbol{f}^{\text{rep}}| = (F + A)\exp(-20s/R)$. The net interparticle force $|\boldsymbol{f}^{\text{net}}| = |\boldsymbol{f}^{\text{att}} + \boldsymbol{f}^{\text{rep}}|$ is repulsive for small separations $s/R < 0.1$, and attractive for $0.1 < s/R < 0.33$. The net attractive force magnitude reaches a maximum of $15\pi\mu L R\dot{\gamma}$ at $s/R = 0.14$. This force is relatively strong; for softwood pulp fibers in a flow where $\mu = 0.1$ Pa · sec and $\dot{\gamma} = 50/\text{sec}$, the corresponding maximum attractive force is 1×10^{-5} N, which is roughly 200 times larger than the measured adhesion force between contacting pulp fibers in water [17].

Simulations of helical fibers with short range attractive forces and no friction develop spatial inhomogeneities in shear flow, as shown in Fig. 8a. The pair distribution function for the fiber CM in Fig. 8b indicates an increased probability of fibers being close together, similar to suspensions with interfiber friction (Fig. 5).

Despite structural similarities between suspensions with attractive and frictional interparticle forces, attractive force flocs are less cohesive—they store essentially no energy upon relaxation of shear, and disperse quickly in unbounded shear flow. Figure 9 tracks the fiber population in a floc that initially contains 80 fibers as it breaks up in unbounded shear flow. For a dimensionless stiffness DS = 0.050, attractive forces delay floc breakup only slightly compared to the case with purely repulsive interfiber forces. Figure 9 also demonstrates that floc coherency increases with decreasing fiber stiffness DS. This behavior differs qualitatively from both experimental observations and simulations of mechanical flocs. Thus,

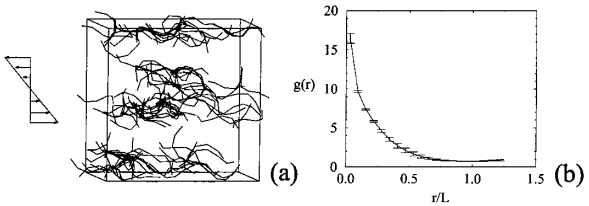

FIG. 8. (a) Suspension structure, (b) fiber CM pair distribution function for 0.125 vol% suspension of helical fibers, $r_p = 70$, DS = 0.050, $\mu_f^{\text{stat}} = 0$, with attractive forces between fibers.

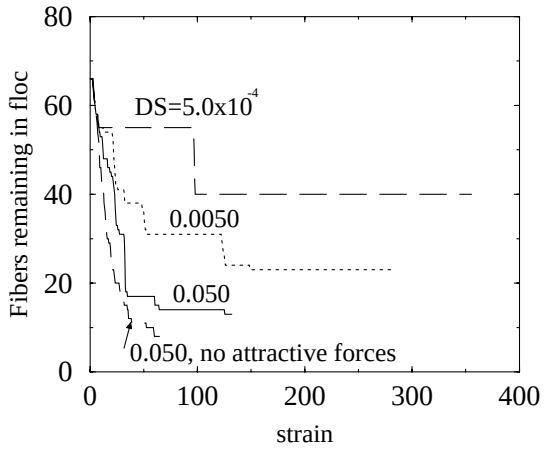

FIG. 9. Fibers remaining in a floc in unbounded shear flow as a function of strain for various fiber stiffnesses: $r_p = 70$, helical fibers, $\mu_f^{\text{stat}} = 0$, attractive interfiber forces except where noted.

our simulations demonstrate the importance of mechanical features, rather than attractive forces, on fiber flocculation.

In conclusion, flocs form in particle level simulations under similar conditions (fiber aspect ratio, concentration, stiffness, equilibrium shape) as in experiments. Flocs form in the absence of attractive forces between particles—interfiber friction and repulsive interactions alone induce flocculation. Simulated mechanical flocs exhibit characteristics consistent with experiments—elastic energy storage upon cessation of shear flow, and increased floc cohesiveness with increased fiber stiffness. Simulated attractive force flocs do not exhibit these characteristics.

While successful, the simulation technique has shortcomings and limitations that should be mentioned. The static friction coefficient of 20 used in simulations is much higher than the experimentally measured value of 0.5 for pulp fiber surfaces [17]. The lack of sliding friction forces in the current model is a possible cause for this discrepancy. The model neglects hydrodynamic interactions between fibers. Existing techniques [18,19] for studying hydrodynamic interactions could be included, at an increased computational cost. Finally, in experiments, flocs grow to be several times larger than the current simulation box size. Extensive computer memory is needed to examine larger, more realistic flow geometries.

[1] K. G. Soga, J. R. Melrose, and R. C. Ball, J. Chem. Phys. **108**, 6026 (1998).
[2] J. Swenson, M. V. Smalley, and H. L. M. Hatharasinghe, Phys. Rev. Lett. **81**, 5840 (1998).
[3] Y. T. Hu, P. Boltenhagen, and D. J. Pine, J. Rheol. **42**, 1185 (1998).
[4] S. G. Mason, TAPPI J. **33**, 440 (1950).
[5] S. G. Mason, Pulp Pap. Can. **55**, 96 (1954).
[6] D. Wahren, in *Proceedings of the Institute of Paper Chemistry Symposium on Paper Science and Technology* (Institute of Paper Chemistry, Appleton, WI, 1980).
[7] C. T. J. Dodson, R. R. Farnood, and S. R. Loewen, APPITA J. **47**, 391 (1994).
[8] R. J. Kerekes, in *Proceedings of the International Paper Physics Conference* (CPPA, Montreal, 1995), p. 23.
[9] R. Meyer and D. Wahren, Svensk Papperstid. **67**, 432 (1964).
[10] K. E. Almin, P. Biel, and D. Wahren, Svensk Papperstid. **70**, 772 (1967).
[11] R. M. Soszynski and R. J. Kerekes, Nord. Pulp Pap. J. **3**, 172 (1988).
[12] C. F. Schmid, L. H. Switzer, and D. J. Klingenberg [J. Rheol. (to be published)].
[13] C. F. Schmid, Ph.D. thesis, University of Wisconsin, 1999.
[14] R. J. Kerekes and P. A. Tam Doo, J. Pulp. Pap. Sci. **11**, J60 (1985).
[15] R. H. Zhao and R. J. Kerekes, TAPPI J. **76**, 183 (1993).
[16] N. Takeuchi, S. Senda, K. Namba, and G. Kuwabara, APPITA J. **37**, 223 (1983).
[17] E. A. Amelina, E. D. Shchukin, and A. M. Parfenova, Coll. J. **60**, 537 (1998).
[18] M. B. Mackaplow and E. S. G. Shaqfeh, J. Fluid Mech. **329**, 155 (1996).
[19] O. G. Harlan, R. R. Sundararajakumar, and D. L. Koch, J. Fluid Mech. **388**, 355 (1999).